METHODS FOR CONSIDERING THE EDDY CURRENT LOSSES IN THE DETAILED MODEL OF A HV-TRANSFORMER

Amir M. Miri M.A. Nothaft P. Braess

Institut für Elektroenergiesysteme und Hochspannungstechnik
Universität Karlsruhe
Kaiserstraße 12 - 76128 Karlsruhe
GERMANY

ABSTRACT

In this work a detailed model is derived for the whole winding system of a high-voltage power transformer. It is based on lumped elements. The network parameters; capacitances, inductances and resitances are determined from the geometric and material data, which are available from construction drawings. In order to get accurate and reliable results from the study of the high-frequency behaviour in the windings, the eddy current losses have to be included. To take into account these losses, two methods are presented. The first one uses in series connected R-L-parallel circuits, the second method includes a time-dependent equivalent resistance connected to a time dependent equivalent voltage source. These time-dependent elements are determined on-line in TACS. In addition, a model with distributed parameters is developed for the investigated power transformer 36/420kV. Each disc of the winding is represented by a transmission-line, whose values per unit length are derived from material data. The mutual inductive coupling between the two discs is realized by using modal analysis.

1 INTRODUCTION

Lightning incidences in high voltage networks and disconnector operations inside air- and SF6-insulated substations result in travelling waves with rise times in the range of ms to ns, which correspond to frequencies in the range of kHz to several MHz. If the dominating frequency of a voltage surge corresponds to one of the natural frequencies of the transformer winding, an excitation of oscillations at parts of the winding can arise. This causes high-voltage stresses, which can lead to a flashover inside the winding. For examination of the resonance processes and voltage shape inside the transformer, a detailed model of the complete winding system with lumped elements is developed in this paper. The occuring electrical and magnetic fields are modeled through an equivalent network consisting of lumped elements and active devices. In order to get accurate and reliable simulation results, the eddy current effects in the transformer winding have to be considered. In this work the magnetic stray-field in the winding block of a transformer has been calculated to determine the resistance increase in the winding. To take the frequency sensitivity of this damping parameter into account, two models for calculations in the frequency and time domain are presented

2 INVESTIGATED TRANSFORMER

The analysis was performed upon a 36/420 kV power transformer whose winding arrangement is displayed in Figure 1. The transformer is composed of a low voltage (LVW), a high voltage (HVW) and a tap winding (TW). The HVW and TW are divided into two parallel symmetrical halves and are constructed as a disc winding. The LVW is designed as a multi-layer winding. Measurements with a lightning impulse voltage (1.2/50 µs) and the LVW short circuited were carried out for two test arrangements (Figure 1).

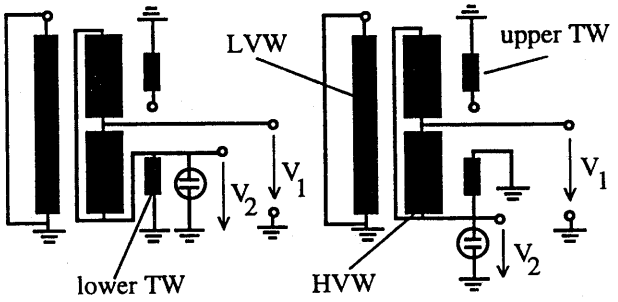

Figure 1: Test arrangement 1 (left) and test arrangement 2 (right)

3 MODELING

The transient and resonance process within the interior of the transformer is defined as a non-linear field problem. This specific problem is dependant upon the complex geometry, the various materials as well as the high-frequency components of the injected voltage.

In order to solve this problem, the electrical and magnetical interactions inside the transformer windings are directed to a corresponding network of lumped elements and active devices. The corresponding simulation model is displayed in Figure 2. The resulting series capacitance of a singular disc unit is described by C_i. The coupling capacitance for the surrounding winding units is decribed by C_{Ki} and the stray ground capacitances by C_{Ei}. The self inductance of an individual disc unit is symbolized by L_i and the coupling inductances which connect to other discs as M_{ik}. The Resistance R_i reproduces the corresponding losses in the copper of the winding and G_i takes the dielectric losses of the insulation into account.

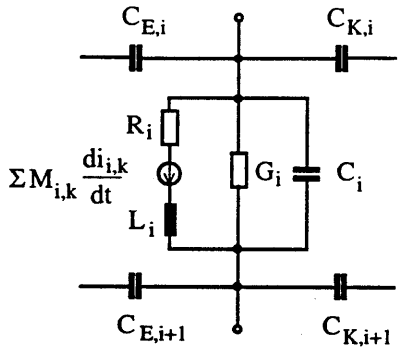

Figure 2: Equivalent network of a singular disc unit

Today, interwound disc coils for voltage linearization are customary. The interwound winding is shown in Figure 3a. Generally, a unit consists of N disc coils (here: N=2) with each n windings and p parallel conductors (here: p=1). Because of the chosen conductor location, the differential voltage between the conductors is increased. This results in higher capacitive energy storage and higher serial capacitance. The capacitances and self-inductances that appear in an interwound winding are also shown in Figure 3b. For clarity, resistances and mutual-inductances have not been depicted.

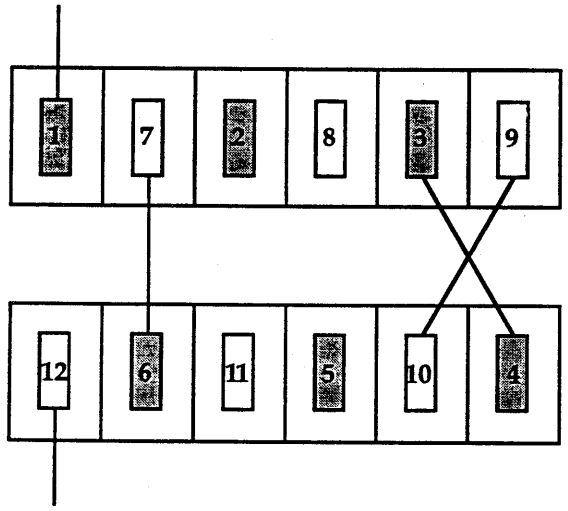

Figure 3a: Interwound disc winding

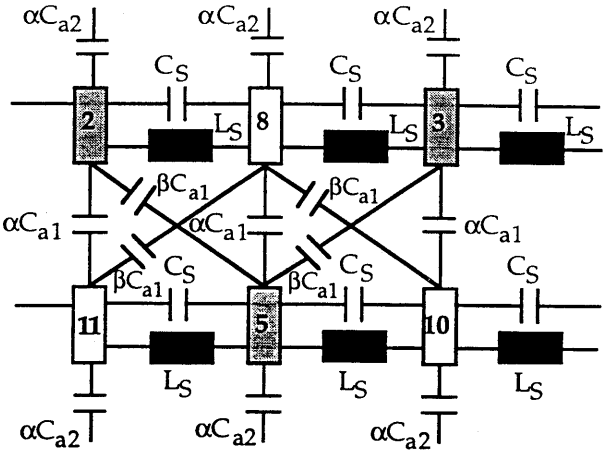

Figure 3b: Capacitance and inductance distribution

In contrast to the non-interwound winding, there is a difference in the electrical potential of the parallel laying turns. The correction factors α and β take into account these changed potential gradings as well as geometrical influence .

3.1 Calculation of the capacitances

The ground capacitances account for the electric fields between disc units and ground, whereas the coupling capacitances account for the electric fields existing between the disc units themselves. With this method it is possible to simulate the displacement current flow in the respective insulations. The insulation between the turns is constructed, as a rule, with multiple layers. These layers consist of oil, transformer board and a mixture of oil and transformer board alternately. The ground and coupling capacitances are provided by help of the following equation:

$$C_E = k_{edge} \frac{\varepsilon_0 \varepsilon_{equi} b \cdot \pi \cdot d_m}{e} \qquad (1)$$

in which k_{edge} specifies the capacitance change due to the "edge" effect, b the height of a conductor, e the distance of the electrodes, d_m the mediating diameter, and ε_{equi} the equivalent dielectric constant of the multi-layered dielectric. The determination of the equivalent capacitance C_{ik} in a disc coil unit provides substantial difficulties, due to the complex structure of such a double coil unit and its capacitances. Figure 4 shows the equivalent arrangement of a normal disc winding with the underlying capacitances.

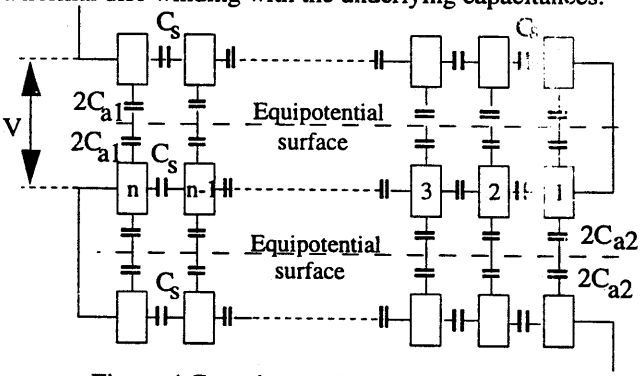

Figure 4 Capacitances in a double coil unit

The resulting series capacitance C_{ik} is composed of four partial capacitances:

C_1: The capacitance produced by the element capacitance C_S between the parallel laying turns of a disc unit.

C_2: The capacitance produced by the element capacitance C_{a1} between the surrounding interturn conductors within the disc unit.

C_3: The capacitance produced by the element capacitance C_{a2} between the surrounding interturn conductors of two succesive disc units.

C_4: The capacitance produced by the element capacitance C_{a3} between the top and bottom ends of the winding which is connected to the shield electrode.

The determination of the capacitances C_i (i=1..4) is carried out by equating the energy saved in C_i (i=1..4) with the sum of the energy which is saved in the corresponding element capacitances C_S, C_{a1}, C_{a2} and C_{a3} respectively. For the interwound disc coil winding of type "Savoisienne" in this power transformer, the application of the energy balance - for an even interturn quantity n - results in the following element capacitances:

$$C_1 = \left(1 - \frac{1}{n} + \frac{5}{4n^2} - \frac{1}{2n^3}\right) \cdot 2nC_S$$

$$C_2 = \left(1 - \frac{3}{20n} - \frac{1}{4n^2}\right) \cdot \frac{5n}{12} \cdot C_{a1} \qquad (2)$$

$$C_3 = \left(1 - \frac{15}{68n} - \frac{5}{68n^2}\right) \cdot \frac{17n}{12} \cdot C_{a2}$$

$$C_4 = \left(1 + \frac{9}{10n} + \frac{1}{5n^2}\right) \cdot \frac{5n}{12} \cdot C_{a3}$$

For an uneven interturn number n, one calculates in a similar manner. The determination of the discrete capacitances C_S and C_a are provided with the help of the following equations:

$$C_S = \left[1 + \frac{d}{b} \cdot \left(0{,}95 + 1{,}2\frac{a}{b} - 1{,}5\frac{d}{b}\right)\right] \cdot \frac{\varepsilon_0 \varepsilon_p b \pi d_m}{c}$$

$$C_a = \left[1 + \frac{c}{a} \cdot \left(0{,}87 + 0{,}03\frac{d}{a} - 0{,}15\frac{c}{a}\right)\right] \cdot \frac{\varepsilon_0 \varepsilon_p a \pi d_m}{d} \qquad (3)$$

a : Width of the conductor
b : Height of the conductor
e : Distance of the electrodes
d_m : Mediate diameter of the disc unit
d : Axial distance of two disc units

3.2 Calculation of the inductances

The knowledge of the iron core flow at higher frequencies is necessary to determine the inductances of the transformer winding /1/. By the observation of transient processes with frequencies above 10 kHz, one recognizes that the eddy currents are so intensive that the field lines are completely displaced from the interior of the iron core. Since the interior core is practically flux free, the field lines do not enter the core interior.
When calculating the self and mutual inductances for these frequencies one can apply the equations for an air-cored reactor. For the self inductance of a disc unit, one applies:

$$L_{self} = L_0 - \Delta \qquad (4)$$

with

$$L_0 = \frac{\mu_0}{4\pi} \cdot w^2 d_m \xi \qquad (5)$$

Δ : Correction factor for the self inductance
ξ : Correction factor
a : Distance between the conductors laying above and below a disc unit
d_m : Mediate diameter of a disc unit
w : Number of turns

One can calculate the mutual inductance M_{ik} of two circular coils by applying the following equation to the radii r_1 and r_2, as well as with the distance x /2/:

$$M_{ik} = \frac{2\mu_0 w_1 w_2 \sqrt{r_1 r_2}}{\sqrt{k_1}} \cdot \left[K(k_1) - E(k_1)\right]$$

$$k_1 = \frac{1 - \sqrt{1 - k^2}}{1 + \sqrt{1 - k^2}} \qquad (6)$$

$$k = \sqrt{\frac{4 r_1 r_2}{(r_1 + r_2)^2 + x^2}}$$

$E(k_1)$ and $K(k_1)$ are the complete elliptical integrals of the first and second classification, w_1 and w_2 are the turns of the coils.

3.3 Calculation of the parallel conductance

The parallel conductances G_{ik} account for the dielectric losses occuring in the insulation material of the transformer. By means of the considered tan δ–measured values /1/ in the individually insulated (frequency dependent) material, one can calculate the parallel value by applying the equation:

$$G_{ik} = 2\pi f \cdot C_{ik} \cdot \tan\delta(f) \qquad (7)$$

3.4 Calculation of the series resistance

In the case of transient phenomena within the transformer, the frequency-dependent losses corresponding to the eddy-currents in the copper winding represent the most significant damping influence. In the simulation model, the losses are considered by means of resistances connected in series to inductances. These resistances are calculated from the shape of the magnetic stray field on the margins of the winding disc. The damping resistance versus frequency for a disc-unit of the high-voltage winding is shown in Figure 5.

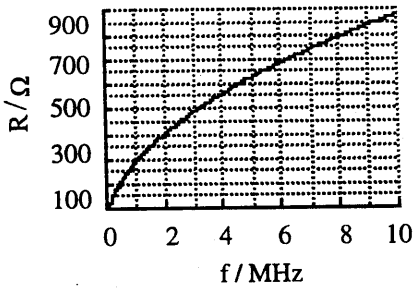

Figure 5: Resistance of the high-voltage winding

4 DETAILED MODEL

With all the discs discretized in the descripted manner one reaches at the single-phase network model of the considered transformer.

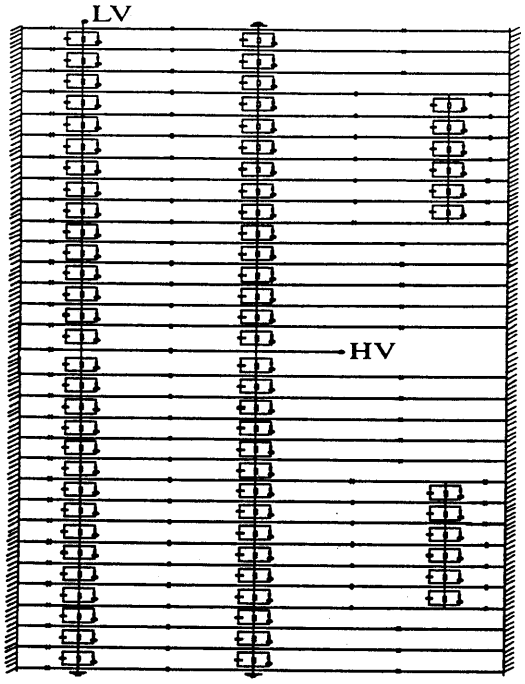

Figure 6: Detailed model of the power transformer

5 MODELLING OF THE FREQUENCY SENSITIVE DAMPING IN THE TIME AND FREQUENCY DOMAIN

For a modeling of the frequency sensitive damping resistances (see 3.4) at simulations in the time and frequency domain, it is necessary to use equivalent networks instead /3,4,5,6/. Various equivalent circuits have been developed to represent the frequency sensitivity of the damping. Two variations of these equivalent circuits are subject of this passage.

5.1 Foster circuits

The first method is based on the Foster circuits that consist of parallel R-L blocks, connected in series. (see Figure 7)

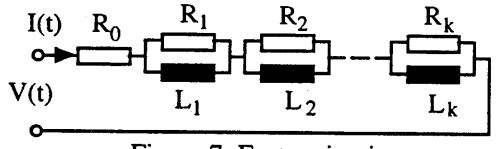

Figure 7: Foster circuit

The real part of the impedance at the terminal has to match the resistance shape in the winding as shown in Figure 6. For this purpose, resistances and inductances, the parameters of this network , have to be determined. The impedance at the terminals of the series Foster circuit shown in Figure 7 is given by

$$Z_{Fk} = R_0 + \sum_{i=1}^{k} \frac{j\omega L_i R_i}{R_i + j\omega L_i} \tag{8}$$

For the real part of this equation we have

$$R_{Fk}(\omega) = R_0 + \sum_{i=1}^{k} \frac{\omega^2 L_i^2 R_i^2}{R_i^2 + \omega^2 L_i^2} = R(\omega) \tag{9}$$

This real part R_{Fk} is determined to match the shape of the series resistance R(ω). Extracting the j th block from the above equation yields:

$$a_j(\omega) = \frac{\omega^2 L_j^2 R_j^2}{R_j^2 + \omega^2 L_j^2} \tag{10}$$

where

$$a_j(\omega) = R(\omega) - R_0 - \sum_{\substack{i=1 \\ i \neq j}}^{k} \frac{\omega^2 L_i^2 R_i^2}{R_i^2 + \omega^2 L_i^2} \tag{11}$$

Evaluating $a_j(\omega)$ at two frequencies ω_{j1}, ω_{j2} we have

$$a_{j1} = a(\omega_{j1}) = \frac{\omega_{j1}^2 L_j^2 R_j^2}{R_j^2 + \omega_{j1}^2 L_j^2}$$

$$a_{j2} = a(\omega_{j2}) = \frac{\omega_{j2}^2 L_j^2 R_j^2}{R_j^2 + \omega_{j2}^2 L_j^2} \tag{12}$$

There exists closed form solution for these equations given by

$$R^2_j = \frac{a_{j1} a_{j2} (\omega^2_{j2} - \omega^2_{j1})}{a_{j1} \omega^2_{j2} - a_{j2} \omega^2_{j1}}$$

$$L_j^2 = \frac{a_{j1}\omega^2_{j2} - a_{j2}\omega^2_{j1}}{\omega_{j1}^2 \omega_{j2}^2 (a_{j2} - a_{j1})} \cdot R_j^2 \tag{13}$$

These equations are used iteratively to calculate the resistances and inductance of the circuit. If all the damping resistances in the network model are replaced by Foster circuits, it is possible to determine the frequency sensitive damping both in time and frequency domain.

5.2 Equivalent time-dependent Thevenin circuits

This second method especially has been put to use for simulations in the time domain with EMTP/ATP.
The Thevenin circuit consists of a time dependent resistor $R_{eq}(t)$ connected in series to a time dependent voltage source $V_{eq}(t)$.

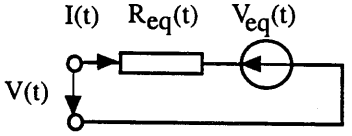

Figure 8: Equivalent time dependent Thevenin circuit

The values of the two components are determined during the calculations in TACS so that the terminal performance of the Thevenin circuit is the same as of the Foster circuit. For the transfer function G(s) we use the transfer function of the Foster circuit $G_{FC}(s)=V(s)/I(s)$.

In our case this function is well-known, because the Foster circuits are available as a network. Finally, the transfer function in the frequency domain has to be determined with the help of the known Foster circuits components. Because of the extensive term this calculation has been carried out with MATHEMATICA /7/. The values for $V_{eq}(t_1)$ and $R_{eq}(t_1)$ can be determined:

$$R_{eq}(t_1) = \frac{2u(t_1) - u(t_1 - \Delta t)}{2i(t_1) - i(t_1 - \Delta t)} \tag{14}$$

$$V_{eq}(t_1) = \frac{u(t_1)\frac{i(t_1 - \Delta t)}{i(t_1)} - u(t_1 - \Delta t)}{2 - \frac{i(t_1 - \Delta t)}{i(t_1)}}$$

6 LINE MODEL REPRESENTATION

In the second part of this work a network model is developed, lossless coupled lines are used to model the winding discs of the transformer. This line model (Figure 9) is developed from the detailled network model which consists only of lumped elements.

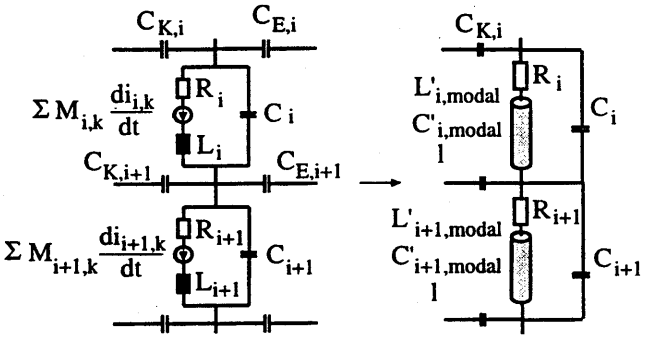

Figure 9: Line model

The π–circuit which consists of stray capacitance $C_{E,i}$, $C_{E,i+1}$ and self-inductance L is replaced by a lossless line. The inductance and capacitance per-unit length of this line results from the equivalent stray capacitance and self-inductance per-unit length of each disc. The discs mutual inductive coupling is realized by coupling the lines in the line modell. The conductance G_i is not considered for simplification. The frequency dependent damping resistance R_i is modeled by Foster circuits. Direct-axis and coupling-capacitancies C_i and $C_{K,i}$ are kept as lumped elements. For transformation of the lines into the modal domain a Fortran program has been developed.

7 COMPARISON OF MEASUREMENT AND SIMULATION RESULTS

In order to prove the detailed model and the modeling of the frequency sensitive damping with Foster and Thevenin circuits, measurement and simulation results are presented. Below, a lightning impulse voltage (1.2/50 µs) was applied to the input of the high voltage winding and the voltage shape at the tap winding was measured.

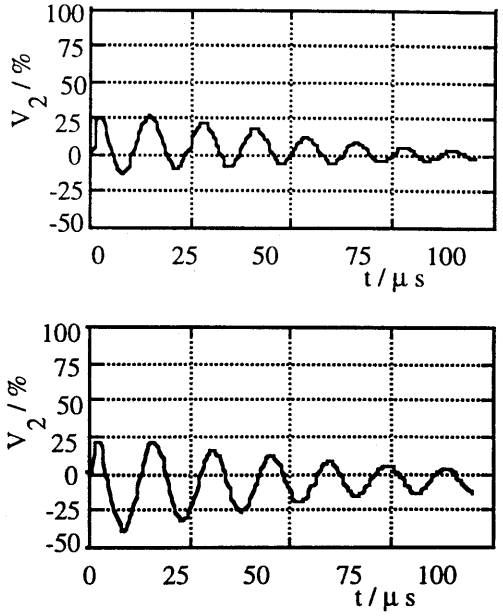

Figure 10: Measurement with test arrangement 1 (above) and test arrangement 2 (below)

In the following, the simulation results with test arrangement 1 and 2 are presented. The plots when using Foster circuits and Thevenin circuits respectively are displayed as an example.

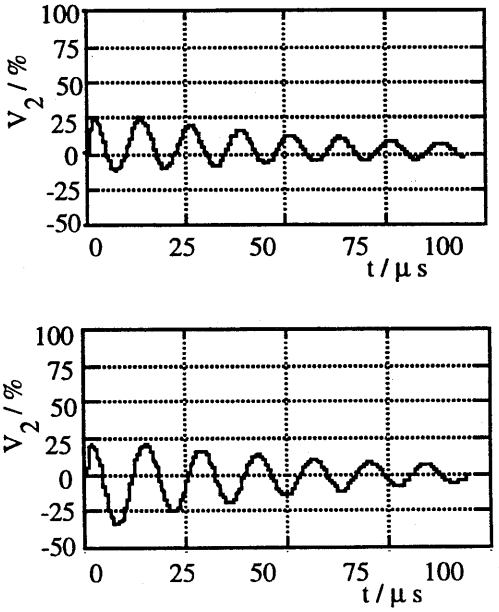

Figure 11: Simulation result with Foster circuits and test arrangement 1 (above); Simulation result with Thevenin circuits and test arrangement 2 (below)

Line model simulations are also calculated. The results show a very close relationship exists.

If a lightning impulse voltage with a very short rising time of approximately 300 ns is applied to the input, the influence of the wave propagation on the line model is significant. Hence the first periods of the oscillation show harmonics of higher order.

Finally, to visualize the resonance frequencies of the 36/420kV power transformer, the transfer function $H(j\omega)=U_2(j\omega)/U_1(j\omega)$ is calculated by using the detailed model /8/.
Fig.12 shows the three-dimensional voltage shape for the HV winding of winding arrangement 1 in the range of 0 kHz up to 200 kHz. Base value for the winding coordinate is the overall length. The input of the high voltage winding is the place 0 in Figure 12, place 1 is the end. The detailed model is excited by an input voltage normalized to the value 1.

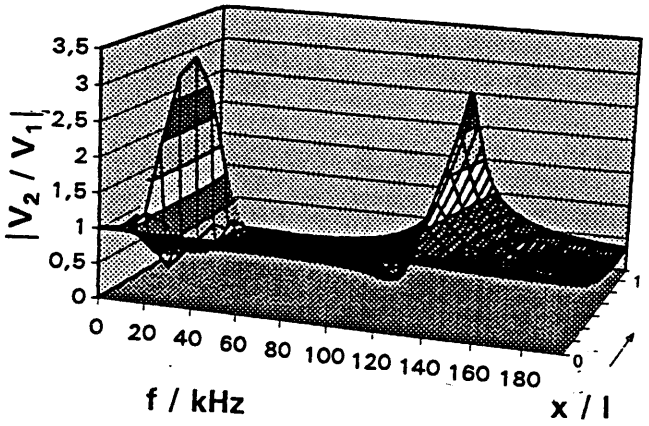

Figure 12: Voltage shape of HV-winding

Fig 13 shows the voltage shape of the tap winding in the range of 0 up to 1.5 MHz. Again, the detailed model is excited by an input voltage normalized to the value 1.
In each plot the calculated frequency response shows two characteristic areas.
The significant point of resonance in both figures at a frequency of approximately 120 kHz occurs due to the junction between HV and the tap winding. Even more clear-cut is the dominant point of resonance at 370 kHz. The voltage peak reaches nearly six times the value of the input voltage. However, the points of resonance in the range between 3 MHz and 5 MHz characterize the oscillations inside the disc unit.

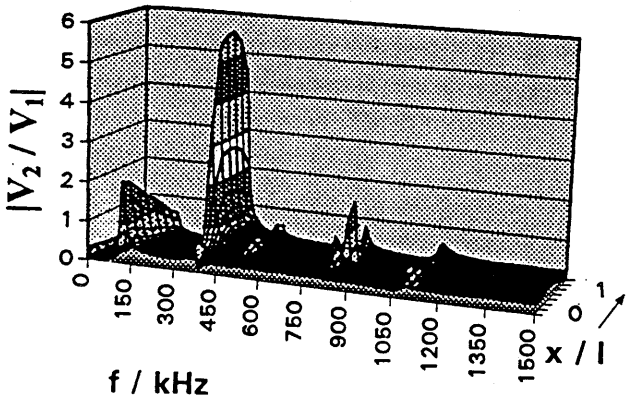

Figure 13: Voltage shape of tap winding

8 CONCLUSION

This paper described a detailed network model of a 36/420 kV power transformer which has been developed from geometrical data. This model enables the investigation of transients inside the transformers disc windings. Two variations of equivalent circuits (Foster/Thevenin) have been presented. These take into account the frequency dependent eddy current losses in the copper winding during simulations in time and frequency domain. In the last part of this paper the transformers discs were modeled as lossless coupled lines. The calculation of this network model took place in the modal domain. Each model has been verified by comparison to existing measurements.

REFERENCES

/1/ Buckow, E.: "Berechnung des Verhaltens von Leistungstransformatoren bei Resonanzanregung und Möglichkeiten des Abbaus innerer Spannungsüberhöhungen"; Dissertation Universität (TH) Darmstadt 1986

/2/ Grover, F.W.: "Inductance Calculations, Working Formulas and Tables-Special Edition prepared for Instrument Society of America"; 1980

/3/ Semlyen, A.; De Leon, F.: "Time Domain Modelling of Eddy Current Effects for Transformer Transients"; IEEE Transactions on Power Delivery, Vol.8,No.1, January 1993

/4/ Leon de, F.; Semelyen, A.: "Efficient Calculation of Elementary Parameters of Transformers"; IEEE Transactions on Power Delivery, Vol.7, Jan. 1992

/5/ Avila-Rosales, J.; Alvarado, F.L.: "Nonlinear Frequency Dependent Transformer Model for the Electromagnetic Studies in Power Systems"; IEEE Transactions on Power apparatus and Systems, Vol. PAS-101, No.11, November 1982

/6/ Menter, F.; Halberschmidt, A.: "Modelling of complex-Valued, Frequency-Dependent Impedance Z(ω) in EMTP"; 18th EMTP Users Group Meeting, May 1990, Marseille, Paper N3/1

/7/ Mathematica Version 2.1; Wolfram Research,Inc./Illinois

/8/ Nothaft, M.: "Untersuchung der Resonanzvorgänge in Wicklungen von Hochspannungsleistungstransformatoren mittels eines detaillierten Modells"; Dissertation Universität Karlsruhe 1994

Adress of author:

Prof. Dr.-Ing. Amir Mansour Miri
Institut für Elekroenergiesysteme u. Hochspannungstechnik
Universität Karlsruhe
Kaiserstraße 12
76128 Karlsruhe - Germany

Fax No.: ++49721-695224
e-mail: miri@ieh.etec.uni-karlsruhe.de